

Variable-Structure Position Control-A Class of Fast and Robust Controllers for Synchronous Reluctance Motor Drives

M. Nabipour¹, H. Abootorabi Zarchi², S. M. Madani³

¹ Faculty of Electrical and Computer Engineering, Isfahan University of Technology, Isfahan-Iran, fl6stinger@gmail.com

² Faculty of Engineering, Ferdowsi University of Mashhad, Mashhad, Iran, zarchih@yahoo.com

³ Faculty of Engineering, University of Isfahan, Isfahan, Iran, madani104@yahoo.com

Abstract — A family of variable structure robust position tracking controller is presented for a three-phase synchronous reluctance motor (SynRM) considering the maximum torque control (MTC) strategy related to this motor. Neglecting the iron losses, the proposed controller is designed including one of the three classes of linear variable structure controller and adaptive input-output feedback linearization (AIOFL) approaches. Foremost, a sliding mode-plus-PI controller is used to obtain the stator current reference signal. For that stage, three classes of a PI-sliding controller are presented. These methods are then compared and its characteristics are specified and the optimum use for any case, determined. The presented position controller is fast response and robust against mechanical parameter uncertainties and load torque disturbance. At Second stage, the proposed sliding mode based AIOFL controller estimates the unknown electrical uncertainties without using sign(.) or sat(.) function. Hence, it reduces chattering or steady state error phenomenon. Finally, the effectiveness and feasibility of the proposed control approach is demonstrated by computer simulation. The results obtained confirm that the desired position reference command is perfectly tracked in spite of motor parameter uncertainties and load torque disturbance.

Keyword: Variable structure. synchronous reluctance machine. position control. adaptive nonlinear control.

I. INTRODUCTION

In recent years, the synchronous reluctance motor (SynRM) received much attention for many applications due to its cold rotor, simple and rugged construction [1-3]. Also it is not based on rare-earth magnets.

In these recent years, the state feedback Linearization and input output feedback linearization have been tested on the motor Drives and have shown satisfying results [4-6]. The basic idea is first to transform the motor nonlinear system into a linear one by a nonlinear feedback, and then use the well-know and powerful linear design techniques to complete the control design. These techniques however, require the full knowledge of motor parameters and load condition with sufficient accuracy [7].

In practice, we don't always have ideal situations, and there always is some uncertainties in parameters, so it's vital to overcome the uncertainties and perturbations. Variable structure control (VSC) is one of the robust control methods applicable to electromechanical systems [8-9]. The uncertainties, parameter variations and/or disturbances can be rejected by variable structure control when the boundaries of the systems uncertainties of lump are known. However, specific and reliable system uncertainty boundaries are difficultly obtained for practical applications. In real applications, uncertainty boundaries can easily exceed the assumed magnitude range, under which the existence-conditions of the sliding mode are broken and control performance deteriorates severely. Using high gain

control to improve disturbance rejection has been proposed. A control system using a large constant gain is simple to implement. However, it produces unnecessary deviations from the switching manifold and causes large amounts of chattering in the control system, which starts to make pulsating torque and damages the rotor structure and collapses the rotor after some time. However, this chattering phenomena can be overcome by replacing the signum function, the one responsible in producing it, by a saturation function which limits the boundaries by nature. On the other hand, steady state error is produced. Hence, in recent years, some researchers [10] proposed the methods to find the uncertainty upper boundaries and reduce the steady state error when the signum function is replaced by the saturation function. Their major concept is to estimate the bounded uncertainties in real-time for the controlled system. Hence, the control signal of the controller is smaller than the conventional sliding mode controller and the chattering phenomenon is also reduced.

To solve the above problem, in this research work, a family of nonlinear position tracking controller is introduced which is including a class of linear variable structure control (LVSC) and adaptive input-output feedback linearization (AIOFL) techniques. The proposed different classes of LVSC position control scheme take advantage of the best features of linear control, smooth operation, and of VSC, robustness to perturbations. There are three classes of LVSC which will be discussed in detail in next sections. Moreover, the proposed sliding mode based AIOFL controller, in electrical part, estimates the unknown uncertainties without using sign(.) or sat(.) function. Hence, it reduces chattering or steady state error phenomenon.

This paper is organized as follows. At first, in Section II, the SynRM model and maximum torque control (MTC) scheme are presented. Secondly, the concepts of LVSC classes used in position control and the theory of an adaptive sliding-mode (SM) position controller are described in Section III. A nonlinear AIOFL controller is designed in Section IV. In Section V, the simulation results obtained confirm that the desired position reference command is perfectly tracked in spite of parameter uncertainties and external load disturbances. Finally, conclusions are given in Section VI.

II. SYNRM MODELING AND MAXIMUM TORQUE CONTROL STRATEGY

The SynRM voltage equations in the rotor d-q axis reference frame are described by [1]

$$V_{ds} = L_d \frac{di_{ds}}{dt} + R_s i_{ds} - \omega_e L_q i_{qs} \quad (1)$$

$$V_{qs} = L_q \frac{di_{qs}}{dt} + R_s i_{qs} + \omega_e L_d i_{ds} \quad (2)$$

$$\lambda_{ds} = L_d i_{ds}, \quad \lambda_{qs} = L_q i_{qs} \quad (3)$$

Where V_{ds} and V_{qs} are the ds -qs axis stator voltages, i_{ds} and i_{qs} are the stator two axis currents, L_d and L_q denote the SynRM inductances and ω_e is the rotor electrical angular velocity.

In addition, the SynRM generated torque is given by

$$T_e = \frac{3P}{2} (L_d - L_q) i_{ds} i_{qs} \quad (4)$$

or

$$T_e = \frac{3P}{4} \{L_d - L_q\} i_s^2 \sin\{2\delta\} \quad (5)$$

Where P is the number of motor poles and δ is the current vector angle with respect to rotor d axis and $i_s = \sqrt{i_{ds}^2 + i_{qs}^2}$,

and

$$\begin{cases} i_{ds} = i_s \cos \delta \\ i_{qs} = i_s \sin \delta \end{cases} \quad (6)$$

Moreover, the associated mechanical equations are as follows

$$J_m \frac{d\omega_m}{dt} + B_m \omega_m = T_e - T_l \quad (7)$$

$$\frac{d\theta_m}{dt} = \omega_m \quad (8)$$

Where J_m is the rotor moment of inertia, B_m is the friction coefficient, θ_m is the rotor displacement angle in mechanical degrees, ω_m is the rotor angular velocity and T_l denotes the motor load torque.

The torque control strategies relating to SynRM are maximum torque control (MTC), maximum power-factor control (MPFC) and maximum rate of change of torque control (MRCTC) and constant current in inductive axis control (CCIAC). In this paper, MTC is adopted for our SynRM torque control scheme, because this torque control mode can be easily implemented independent on SynRM inductances and has the property of maximum torque per Ampere generation. A brief review of MTC strategy is given below.

In MTC strategy, the current angle δ is set 45° . Since $\sin(2\delta) = \sin(90^\circ) = 1$, (5) becomes

$$T_e = \frac{3P}{4} (L_d - L_q) i_s^2 = K_T i_s^2 \quad (9)$$

where $K_T = \frac{3P}{4} (L_d - L_q)$. Note that $i_{ds} = i_{qs}$ for MTC mode, so

$$i_{ds} = \frac{\sqrt{2}}{2} i_s \quad (10)$$

It can be seen that if the MTC torque control strategy is used, one has only to control the angle and magnitude of the current vector to match the desired torque.

III. LINEAR VARIABLE STRUCTURE POSITION CONTROL

To overcome the sudden perturbations, inserted on the setup, we split the plant into two types of series working parts. One part is responsible for mechanical perturbations, the generating of the reference currents and the other one, is set to overcome the electrical perturbations. LVSC is used in the 1st part and adaptive robust IOFL is used in the 2nd part. As mentioned before, there are three classes of LVSC schemes which are used according to customer demands.

A. CLASS I

This class is depicted in Fig. 1. It consists of a linear controller that operates in parallel with a sliding-mode one. This controller is a generalized and flexible scheme which takes advantage of the best features of linear control, smooth operation, low physical noise, a less pulsating torques in practice and of VSC, fast response and robustness to perturbations and modeling uncertainties.

The sliding surface S is selected so as to impose sliding-mode operation with first-order dynamics

$$S = K e_\theta(t) - e_\theta(0) + K' e_\omega + K_\theta \int_0^t e_\tau(\tau) d\tau + K_\omega \int_0^t e_\omega(\tau) d\tau \quad (11)$$

Where all the coefficients are selected to match the desired behaviors. The proposed controller (11) produces the stator current reference signal as following

$$i_s^* = (K_p + K_I / s) (K_1 e_\theta + K_2 e_\omega) (\text{sgn}(S)) \quad (12)$$

where K_p and K_I are the PI controller gains and K_1 and K_2 are constants. The LVSC employs a switching component and a linear one. During the transient state, the $e_\theta^* \text{sgn}(\cdot)$ is dominant. In this case, the sliding part is dominant and the sliding ripple depends on e_θ . In the steady-state, errors are very small and the $e_\theta^* S$ is close to zero so the switching surface doesn't change much so the PI controller input turns to e_θ and a semi PI behavior is expected. Adequate balance between linear and switching behavior is easily achieved by proper gain selection. PI gains are selected so that the linear control provides the desired steady state dynamic response, while the VSC gains determine the robustness in dynamic operation. The VSC design procedure [7] requires the gains to be large enough in order to compensate for modeling uncertainties and perturbations. In this case, the K_1 & K_2 gains are selected as large as needed to obtain the desired performance in terms of robustness and chattering.

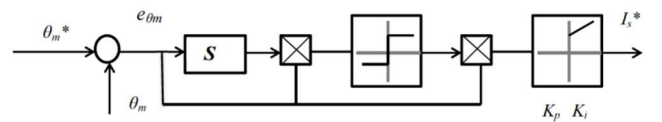


Fig1: Linear and Variable Structure Control (LVSC class I) Block Diagram

B. CLASS II

This controller has a rather similar structure, but shows slightly different results in behavior. This strategy, works in such a way, that ,for initial states where perturbation is inserted, while the ERROR is dominant, it acts as a linear (PI) controller, so we should expect that the controller will start to follow the trajectory smoothly, but slowly . Then, when the ERROR is small enough, the VSC is dominant and the sliding mode controller takes over the control. From now, a robust operation with chattering is expected.

Designing the controller starts with determining the sliding surface which is selected as the sliding surface in class I. The reference current is different and is selected as following

$$i_s^* = (K_p + K_I / s) (K_1 e_\theta + K_2 e_\omega + K_{VSC} \text{sgn}(S)) \quad (13)$$

Similar to the last controller, the methods of selecting the gains are the same.

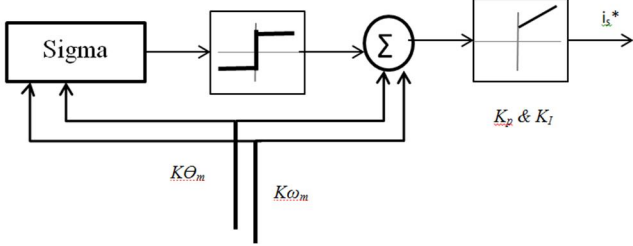


Fig2: Linear and Variable Structure Control (LVSC class II) Block Diagram

C. CLASS III

This method is the simplest method among all LVSC approaches. It acts like the bang bang or Hysteresis control, meaning, when S is positive, PI increases the I_s^* and when S is negative, it reduces I_s^* .

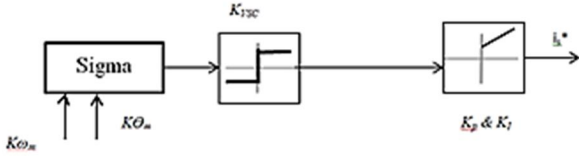


Fig3: Linear and Variable Structure Control (LVSC class III) Block Diagram

IV. ADAPTIVE ROBUST IOFL

In this section, a nonlinear adaptive robust controller is designed based on combination of input-output feedback linearization (IOFL) control and adaptive sliding mode technique.

According to (1-3), the nonlinear SynRM electrical model is described by

$$\dot{i}_d = -a_1 i_d + a_4 \omega_e i_q + a_6 u_d \quad (14)$$

$$\dot{i}_q = -a_2 i_q - a_3 \omega_e i_d + a_7 u_q$$

$$\text{Where } a_1 = \frac{R_s}{L_d}, \quad a_2 = \frac{R_s}{L_q}, \quad a_3 = \frac{L_d}{L_q}, \quad a_4 = \frac{L_q}{L_d},$$

$$a_6 = \frac{1}{L_d} \text{ and } a_7 = \frac{1}{L_q}.$$

Assume that

$$e_d = i_{ds}^* - i_{ds}, \quad e_q = i_{qs}^* - i_{qs} \quad (15)$$

From (14), it is resulted that

$$\dot{e}_d = \dot{i}_{ds}^* - \dot{i}_{ds}, \quad \dot{e}_q = \dot{i}_{qs}^* - \dot{i}_{qs} \quad (16)$$

Substituting (13) into (15) gives

$$\dot{e}_d = \dot{i}_{ds}^* + a_1(i_{ds}^* - e_d) - a_4 \omega_m(i_{ds}^* - e_d) - a_6 u_d \quad (17)$$

$$\dot{e}_q = \dot{i}_{qs}^* + a_2(i_{qs}^* - e_q) - a_3 \omega_m(i_{ds}^* - e_d) - a_7 u_q$$

One can rewrite (16) in the following form

$$\dot{e}_d = -a_{10} e_d + a_{40} \omega_m e_q - a_{60} [\bar{u}_d + P_d(t)] \quad (18)$$

$$\dot{e}_q = -a_{20} e_d - a_{30} \omega_m e_q - a_{70} [\bar{u}_q + P_q(t)]$$

Where $a_i = a_{i0} + \Delta a$ and

$$\bar{u}_d = u_d + (-a_{10} i_{ds}^* + a_{40} \omega_m i_{qs}^* - \dot{i}_{ds}^*) \frac{1}{a_{60}}$$

$$\bar{u}_q = u_q + (-a_{20} i_{ds}^* - a_{30} \omega_m i_{ds}^* - \dot{i}_{qs}^*) \frac{1}{a_{70}} \quad (19)$$

$$P_d(t) = (\Delta a_1(i_{ds}^* - e_d) - \Delta a_4 \omega_m(i_{qs}^* - e_q) - \Delta a_6 u_d) \left(-\frac{1}{a_{60}} \right)$$

$$P_q(t) = (\Delta a_2(i_{qs}^* - e_q) + \Delta a_3 \omega_m(i_{ds}^* - e_d) - \Delta a_7 u_q) \left(-\frac{1}{a_{70}} \right)$$

Now, we define two switching surfaces in the following way

$$s_d = e_d(t) - e_d(0) + c_1 \int_0^t e_d(\tau) d\tau \quad (20)$$

$$s_q = e_q(t) - e_q(0) + c_2 \int_0^t e_q(\tau) d\tau \quad (21)$$

Choosing a Lyapunov function candidate V_3 as

$$V_3 = \frac{1}{2} s_d^2 + \frac{1}{2} s_q^2 \quad (22)$$

The derivative of V_3 with respect to time is

$$\begin{aligned} \dot{V}_3 &= s_d \dot{s}_d + s_q \dot{s}_q \\ &= s_d (\dot{e}_d + c_1 e_d) + s_q (\dot{e}_q + c_2 e_q) \\ &= s_d (-a_{10} e_d + a_{40} \omega_m e_q - a_{60} \bar{u}_d - a_{60} (\tilde{P}_d + \hat{P}_d) + c_1 e_d) \\ &\quad + s_q (-a_{20} e_d - a_{30} \omega_m e_d - a_{70} \bar{u}_q - a_{70} (\tilde{P}_q + \hat{P}_q) + c_2 e_q) \end{aligned} \quad (23)$$

Where $\tilde{P}_d = P_d - \hat{P}_d$ and $\tilde{P}_q = P_q - \hat{P}_q$

\hat{P}_d and \hat{P}_q are the estimated values of the lumped

uncertainties and \tilde{P}_d and \tilde{P}_q are the estimated errors between the actual values and the estimated values of the lumped uncertainties. $P_d(t)$ and $P_q(t)$ are assumed to be constant during the sampling time.

Therefore, the new candidate function is introduced by

$$V_4 = \frac{1}{2} s_d^2 + \frac{1}{2} s_q^2 + \frac{1}{2\gamma_d} \tilde{P}_d^2 + \frac{1}{2\gamma_q} \tilde{P}_q^2 \quad (24)$$

Where γ_d and γ_q are positive constants. The derivative of

V_4 can be written as follows

$$\begin{aligned}
\dot{V}_4 &= s_d \dot{s}_d + s_q \dot{s}_q + \frac{1}{\gamma_d} \tilde{P}_d \dot{\tilde{P}}_d + \frac{1}{\gamma_q} \tilde{P}_q \dot{\tilde{P}}_q \\
&= -K_d s_d^2 + s_d (-a_{10} e_d + a_{40} \omega_m e_q - a_{60} \bar{u}_d - a_{60} \hat{P}_d + c_1 e_d + K_d s_d) \\
&\quad - K_q s_q^2 + s_q (-a_{20} e_q - a_{30} \omega_m e_d - a_{70} \bar{u}_q - a_{70} \hat{P}_q + c_2 e_q + K_q s_q) \\
&\quad - \tilde{P}_d \left(\frac{1}{\gamma_d} \dot{\tilde{P}}_d + a_{60} s_d \right) - \tilde{P}_q \left(\frac{1}{\gamma_q} \dot{\tilde{P}}_q + a_{70} s_q \right)
\end{aligned} \quad (25)$$

Where K_d and K_q are positive constants. By selecting $c_1 = a_{10}$ and $c_2 = a_{20}$, one can choose control inputs as

$$\begin{aligned}
\bar{u}_d &= \left(a_{40} \omega_m e_q - a_{60} \hat{P}_d + K_d s_d \right) \frac{1}{a_{60}} \\
\bar{u}_q &= \left(-a_{30} \omega_m e_d - a_{70} \hat{P}_q + K_q s_q \right) \frac{1}{a_{70}}
\end{aligned} \quad (26)$$

One can obtain

$$\begin{aligned}
\dot{V}_4 &= -K_d s_d^2 - K_q s_q^2 \\
&\quad - \tilde{P}_d \left(\frac{1}{\gamma_d} \dot{\tilde{P}}_d + a_{60} s_d \right) - \tilde{P}_q \left(\frac{1}{\gamma_q} \dot{\tilde{P}}_q + a_{70} s_q \right)
\end{aligned} \quad (27)$$

The derivative of the estimated values \hat{P}_d and \hat{P}_q can be expressed by

$$\begin{aligned}
\dot{\hat{P}}_d &= -\gamma_d a_{60} s_d \\
\dot{\hat{P}}_q &= -\gamma_q a_{70} s_q
\end{aligned} \quad (28)$$

Substituting (26) into (25), \dot{V}_4 is

$$\dot{V}_4 = \left(-K_d s_d^2 - K_q s_q^2 \right) \leq 0 \quad (29)$$

One can easily see that according to Barbalet lemma [7], $s_d(t), s_q(t) \rightarrow 0$ as $t \rightarrow \infty$ and also current errors $e_d(t), e_q(t) \rightarrow 0$ as $t \rightarrow \infty$.

V. SIMULATION RESULTS AND DISCUSSION

Based on our control scheme described in this paper, the overall block diagram of SynRM drive is depicted in Fig. 4. From this figure one can see that the proposed nonlinear controller generates the reference voltage vector of a two-level SV-PWM inverter that feeds motor. To show the validity of the presented method, computer simulation is carried out under maximum torque control strategy related to this motor. A C++ step by step computer program was developed to model the drive system control of Fig.4. In this program, the system dynamic equations are solved by a static Range-Kutta fourth order method. In our proposed control approach the system controller gains are obtained by trial and error method. In Fig.5, assuming a cosine position reference signal, the simulation results are shown for MTC strategy corresponding to a three-phase SynRM with the parameters given in Table 1. Load torque, T_1 , is changed at $t=5$ sec from 0.5 N.m into 4 N.m. As shown in this figure, the position as well as the calculated speed reference signal is perfectly tracked in presence of load torque step change. As expected, the two-axis stator currents, i_{ds} and i_{qs} , are the same in Fig.5 for MTC scheme. In order to show the proposed position controller is robust against electrical and

mechanical parameter uncertainties, at $t=8$ s, d-axis inductance and stator resistance have been changed into $L_d = 0.5 * L_{dn}$ and $R_s = 2 * R_{sn}$, as well as at $t=12$ s, the mechanical parameters have been modified to $J_m = 2 * J_{mn}$ and $B_m = 2 * B_{mn}$, where subscript n refers to nominal values. In addition, Simulated results obtained is illustrated in Fig. 6. In this test, load torque is assumed a constant value. From these results a perfect tracking control can be recognized for the position, speed and two-axis currents in spite of motor parameter uncertainties.

In Fig.7. the second and in Fig. 8. the third class of this controller were examined.

As we saw, any of these controllers has its own characteristic which comes handy in certain situations. All of the mentioned methods are robust and can track the trajectory in a suitable manner. But the difference is observable in practice.

All of these methods were put to simulations and the results were a little different from each other. While testing the 1st class in practice, on a SynRM drive, we recognized that after perturbation was introduced, the machine, started to go after the trajectory by a fast and sudden paste, but after reaching the desired trajectory, it showed a soft following behavior which is due to the linearity of the PI controller. On the other hand, after perturbation, the 2nd controller started to go after the trajectory in a slower and smoother manner, but after reaching the desired trajectory, showed some chattering, although very little, but still sensible. This was due to the VSC characteristic of the proposed controller. The 3rd controller is the simplest of all which is suggested for those who or when the dynamic behavior (not in detail), doesn't differ much and just need the motor follow the given trajectory.

So, when you need a controller to follow a desired trajectory fast and act without chattering as well as smooth in steady state, it is recommended to use class I of the presented controllers. Obviously the rotor structure for these occasions should be strong and able to tolerate the produced sudden torques. Otherwise Class II is preferred when the transient behavior is more important while class III is suggested in view point of control.

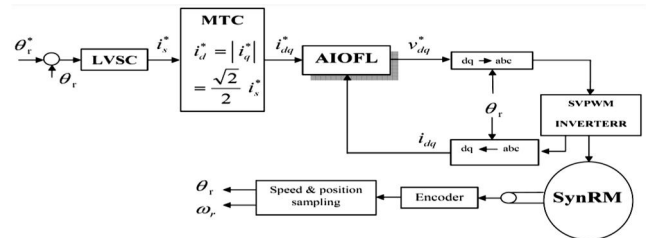


Fig. 4: Overall block diagram of SynRM drive system position control
Table.1: Motor Nominal characteristics

Table 1 motor parameters

$P_n = 1 kW$	$V_n = 230$
$R_s = 2.95 \Omega$	$L_d = 232 mH$
$T_{en} = 5.5 N.m$	$f_n = 60 Hz$
$J_m = .015 Kg.m^2$	$B_m = .003 Nm/rad/sec$
$I_n = 7 A$	$P_p = 2$
$L_q = 118 mH$	

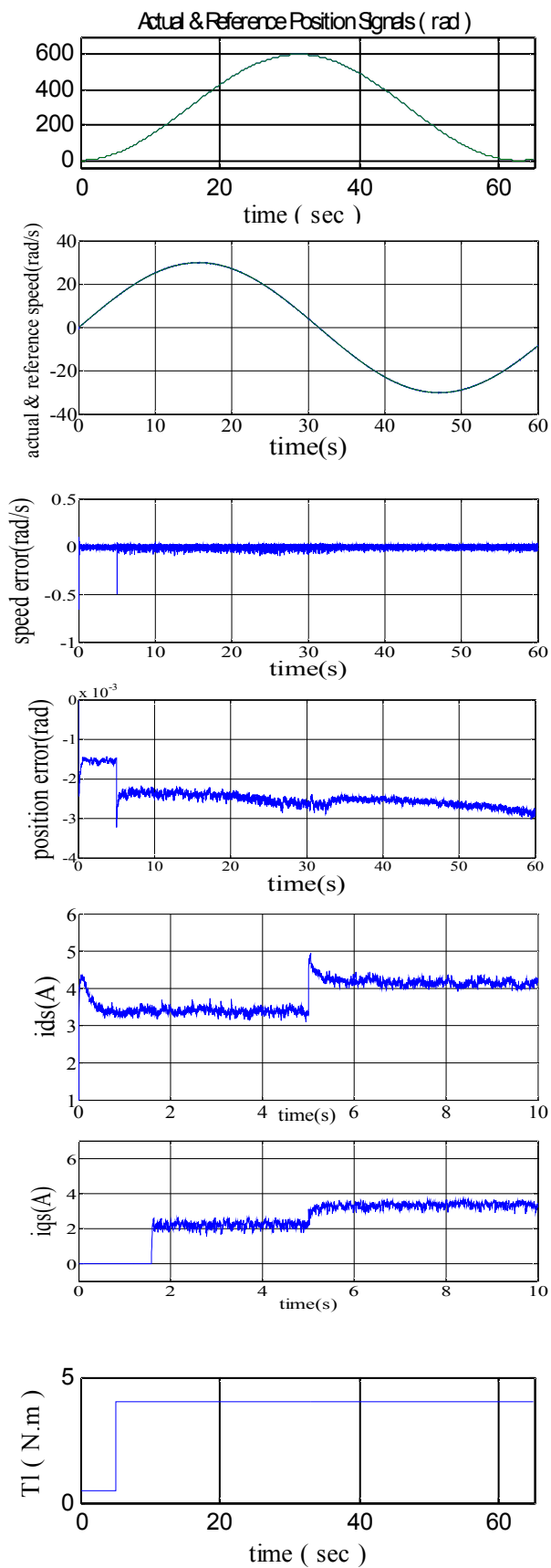


Fig. 5: Simulation Results of the Proposed Position Controller (class I) with mechanical perturbation

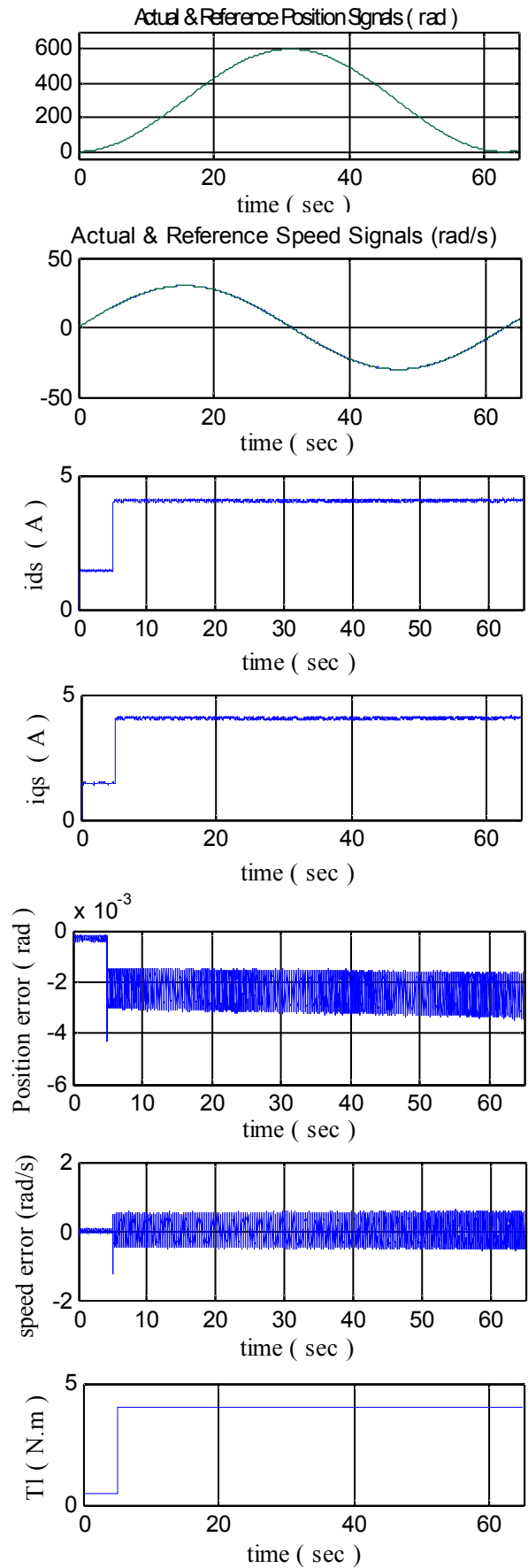


Fig. 7: Simulation Results of the Proposed Position Controller (class II) with mechanical perturbation

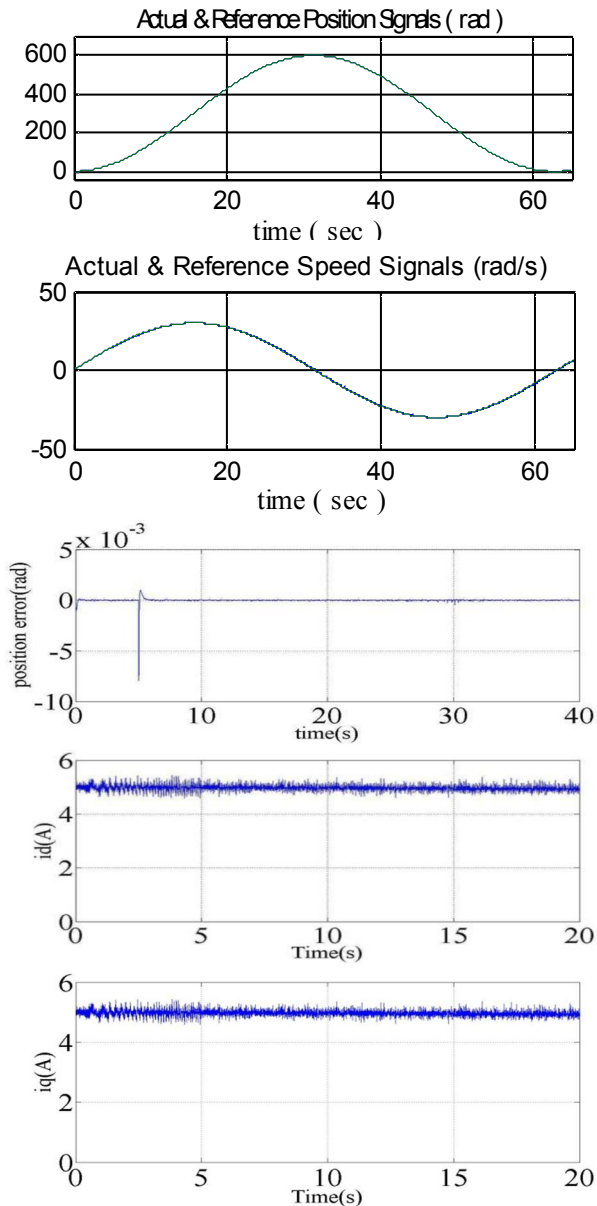


Fig. 8: Simulation Results of the Proposed Position Controller (class III) with mechanical perturbation

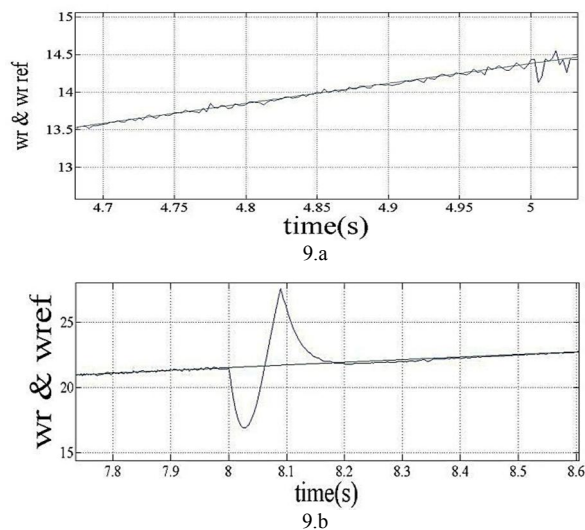


Fig 9 simulation result in case of significant load change

a: (class I)
b: (class II)
c: (class III)

VI. CONCLUSION

Three nonlinear adaptive robust position tracking controllers have been presented for a three-phase synchronous reluctance motor (SynRM) considering the maximum torque control scheme related to this motor. The differences of behavior of these controllers were pointed out. Ignoring the motor iron losses, the proposed controllers have been designed based on combination of linear variable structure technique (in mechanical part) and sliding mode based adaptive input-output feedback linearization (AIOFL) control approach (in electrical part). The proposed AIOFL controller estimates the unknown uncertainties without using $\text{sign}(\cdot)$ or $\text{sat}(\cdot)$ function. Hence, it reduces chattering or steady state error phenomenon. In addition, in order to make the drive system robust to mechanical parameter uncertainties and load torque disturbance, the stator current reference signal was predicted by PI-sliding mode controllers (LVSC). as shown in the simulation results, The proposed robust position controller, is totally robust against electromechanical parameter uncertainties.

REFERENCES

- [1] T. A. Lipo, "Synchronous Reluctance Machines- A Variable Alternative for AC Drives" *Elect. Machines and Power Sys.*, Vol. 19, pp. 659-671, 1991
- [2] A. Chiba and T. Fukao, "A Closed-loop Operation of Super High-Speed Reluctance Motor for Quick Torque Response", *IEEE Trans. On Industry Application*, vol. 28, No. 3, pp. 600-606, 1992
- [3] T. Matsuo and T. A. Lipo, "Field Oriented of Synchronous Reluctance Motor", *IEEE Trans. On IAS Ann. Meet.* pp. 672-678, 1993.
- [4] T.S. Eldin, W. Dunnigan, J.E. Fletcher, and B.W. Williams, "Nonlinear robust control of a vector-controlled synchronous reluctance machine", *IEEE Trans. Power Electron.*, 1999, 14, (6), pp. 1111-1121
- [5] H. D. Lee, S. J. Kang and S. K. Sul, "Efficiency-Optimized Direct Torque Control of Synchronous Reluctance Motor Using Feedback Linearization," *IEEE Trans. on Industrial Electronics*, vol. 46, No. 1, pp 192-198, 1999
- [6] H. Abootorabi Zarchi, J. Soltani, and Gh. Arab Markadeh, "Adaptive Input-Output Feedback-Linearization-Based Torque Control of Synchronous Reluctance Motor Without Mechanical Sensor", *IEEE Trans. on Ind. Electronics.*, vol. 57, no. 1, pp. 375-384, Jan. 2010.
- [7] R. Marino and P. Tomei, *Nonlinear Control Design*, Prentice Hall, Inc, 1995.
- [8] V. I. Utkin, J. Guldner and J. Shi, *Sliding Mode Control in Electromechanical Systems*, Taylor & Francis, July 1999.
- [9] K. K. Shyu, C. K. Lai and Y. W. Tsai, "Optimal Position Control of Synchronous Reluctance Motor Via Totally Invariant Variable Structure Control", *IEE Proceedings-control Theory and Applications*, Vol. 147, No.1, pp. 28-36, 2000.
- [10] F. J. Lin, S. L. Chiu and K. K. Shyu, "Novel Sliding Mode Controller for Synchronous motor drives", *IEEE Trans. On Aerospace and Electronics*, Vol. 47, No.2, pp. 356-367, 2000.
- [11] C. A. Chen, H. K. Chiang and B. R. Lin, "The Novel Adaptive Sliding Mode Control for Current Sensorless Synchronous Reluctance Motor Speed Drive", China, ICIT 2008.